Jour. Fac. Sci., Hokkaido Univ., Ser. IV,
vol. 18, no. 3, Mar., 1978, pp. 491-505.

MICROFRACTURE IN PEBBLES OF THE UTARO CONGLOMERATE, HOKKAIDO
PART I – OBSERVATION UNDER SCANNING ELECTRON MICROSCOPE

by

Tsuyoshi Uda

(with 13 text-figures)

(Contribution from the Department of Geology and Mineralogy,
Faculty of Science, Hokkaido University, No. 1550)

Abstract

The axial-ratio of limestone and granite pebbles in the Utaro Conglomerate differs from the result of three-axial compressive tests. Observation of the fracture surface by S.E.M. revealed that the intragranular and intergranular normal ruptures develop in the limestone pebbles. On the contrary, in the granite pebbles many types of fracture are observed. If the difference of their initial states is negligible, the propaganda of fracture can be discussed by assuming the condition under which the applied stress remains constant.

In the case of limestone, the apicies of fractures look stair-like form due to generation of *punched* dislocation. This phenomenon probably indicates that the critical strength is smaller than E/10 and plastic relaxation is generated at the apicies of fractures. On the contrary, the granite pebble behaves as a brittle (i.e. $\sigma_c \gg E/10$), and is deformed elastically during stress acted. Therefore, the fractures are well developed and megascopical axial-ratio is increased.

Introduction

The Utaro Conglomerate near the Cape Erimo, southern end of central Hokkaido, is famous for the deformed granite pebbles which are extremely elongated. It is noted that the pebbles of different lithology have different axial-ratio, though the general stresses acting on them should have been equal throughout the conglomerate layer. The deformed granite pebbles attain up to 12 in axial-ratio (the maximum value; the longest axis of pebble is divided by the shortest one), whereas the limestone pebbles are generally small in this ratio (Uda, 1973, 1976). This phenomenon contradicts to the result of three-axial compression tests on granite and limestone.

In general, since granite has low ductility and higher yield strength, it must be easily destructed under higher differential-stress. On the other hand, limestone has high ductility and low yield strength. Accordingly, the generation of flowage is apt to occur rather than break down. From these facts, it is expected that the axial ratio of granite pebble is smaller than that of limestone. This

notable difference in the axial-ratio between field occurrence and three-axial test attracts our attention.

According to the fracture mechanics of structural materials (Telelman and McEvily, 1967), a specific type of fracture has a characteristic pattern on the surface. By means of observation of this characteristic pattern, it is possible to restore the fracturing process and also to estimate the cause of fracturing.

In order to clarify the problem mentioned above, the scanning electron microscope observation was carried out, and the formation mechanism of fracturing pattern is discussed in this paper.

Types of Fracture

On the basis of fracture mechanics, it is possible to decide condition of nominal fracture strength, length of fracture, and fracture toughness (i.e. the critical elastic work with an unstable fracturing). Types of fracture are classified as follows;

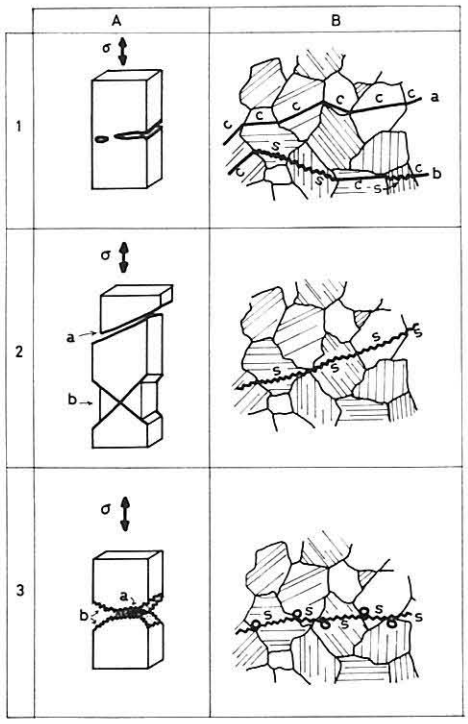

Fig. 1 Megascopic (A) and microscopic (B) fractures. 1. Cleavage fracture; a.continuous cleavage fracture, b.discontinuous cleavage fracture, 2. Shear fracture; a.slant-shear fracture, b.chisel-point fracture, 3. Normal (a) and shear (b) ruptures.

(1) Cleavage fracture (Fig. 1, 1) – This type forms when the cleavage crack develops within the material subjected to tensile component of external stress. As shown in Fig. 1 (1, 8-a) the continuous cleavage fracture forms when the bond of every grains are failed to be normal to the fracture plane. The discontinuous cleavage fracture (1, B-b) generates when cleavage fractures develop in some grains and shear failures in other grains.
(2) Shear fracture (Fig. 1, 2) – This type generates when the atomic bond of material is failed parallel to the fracture plane. The slant-fracture generates parallel to interface of material. The chisel-point fracture occurs due to the shear in two directions.
(3) Normal and shear ruptures (Fig. 1, 3) – Trace of fracturing is normal to the tensile stress, but marked notches are observed on the fracture surface under the S.E.M. The fracture is developed by the connection of boids. Each boid is shear failure found within the fracture plane and slants 30° – 45° to the tensile stress.

Under certain condition, the boundaries between neighbouring grains in polycrystalline aggregate are weaker in coherence than the intragranular surface. In this case, fracturing occurs rather on the grain boundaries than in the intrior of grain. Accordingly, fractures can be classified into the following six types; (i) intragranular cleavage fracture, (ii) intragranular shear fracture, (iii) intragranular normal rupture, (iv) intergranular cleavage fracture, (v)

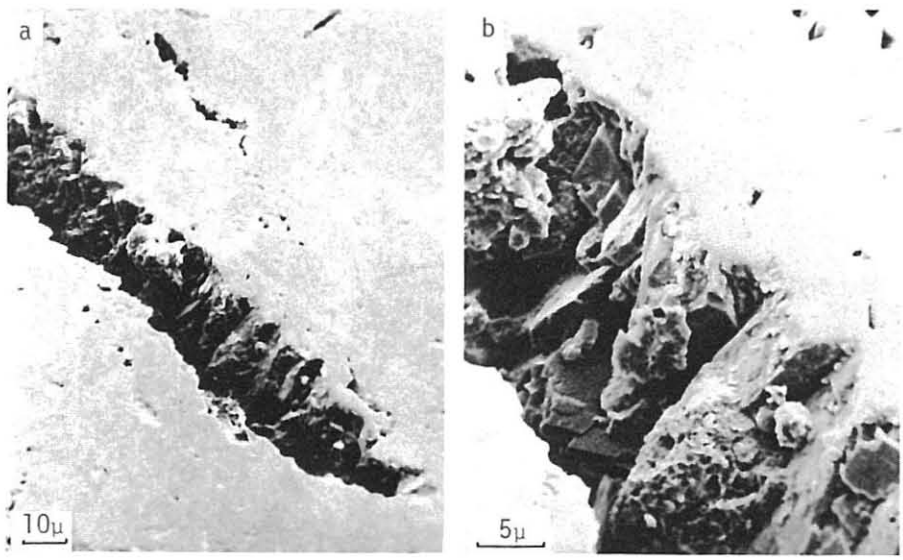

Fig. 2 Normal rupture in limestone pebble. A fracture with marked notches plane (a), and mutually crossed planes (b).

intergranular shear fracture, and (vi) intergranular normal rupture. Each type of fractures produces depending upon the environmental condition and state of nominal stress and strain.

Method

Pebble specimen were cut into thin slabs, 1 x 1 cm square. These slabs were embedded in epoxy resin and polished with #3000 abrasive and finally chrome-oxide abrasive on woolen cloth. These samples were rinsed with distilled water and dried.

The polished limestone was immersed into 20°C, 10% hydrochloric acid for 20 seconds, and the granite was immersed into 20°C, 10% hydrofluoric acid for a few seconds (Minoura, 1975). After etching all samples were immediately rinsed with distilled water, and completely dried. Then, the carbon coating and gold shadowing were treated by the vacuum evaporation apparatus, JEOL LEE-4B. Observation was made using a JEOL JSM-S1 scanning election microscope in Historical Museum of Hokkaido.

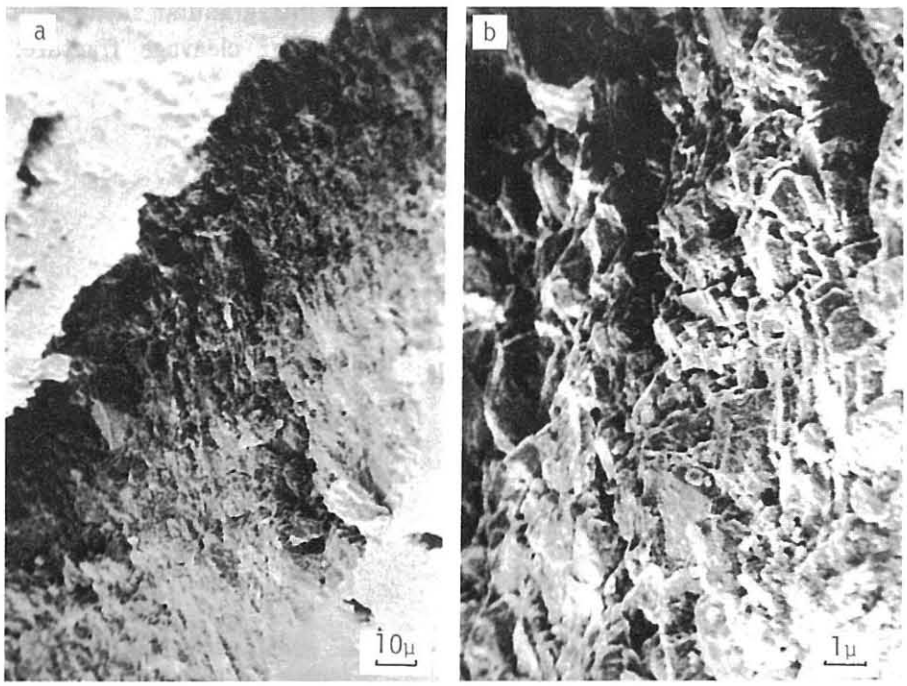

Fig. 3 Fracture surface in limestone (a), and the crystallographic from of calcite on the fracture surface (b).

Observation of Fracture

Limestone Pebble

Most of the fractures are intragranular and intergranular normal ruptures. Calcite has a perfact rhombohedral cleavage $\{10\bar{1}1\}$, and sometimes parting is parallel to $\{0\bar{1}12\}$ which is due to twin-griding. The fracture propagates not only in the same direction as megascopic fracture but also in the opposite direction. The fracture detours around the grain as an intergranular fracture, where the crystallographic cleavage plane crosses the direction of fracture. The fracture observed under the S.E.M. has a certain width and its plane is notched (Fig. 2a). Under higher magnification, the minute planes of notches cross obliquely each other (Fig. 2b). Boids are formed when no fracture is developed. The crystallographic form of calcite observed on the fracture surface under further higher magnification is shown in Fig. 3. Fig. 4a shows fractures of which apicies do not reach the neighbour one. The apex of fracture looks stair-like form due to the heterogeneous generation of *punched* dislocation loop, and many smaller pits by dislocation were observed around the apex (Fig. 4b). These phenomena probably suggest that the plastic relaxation of strain occurs at the apex of fracture.

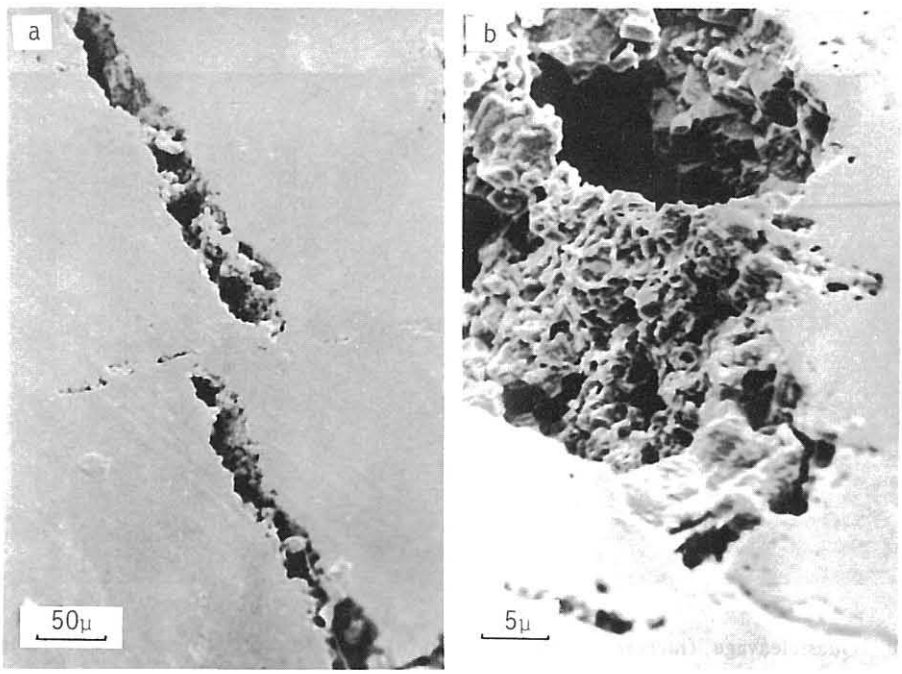

Fig. 4 Apicies of fractures which do not reach the neighbour (a), and the stair-like form of apex (b).

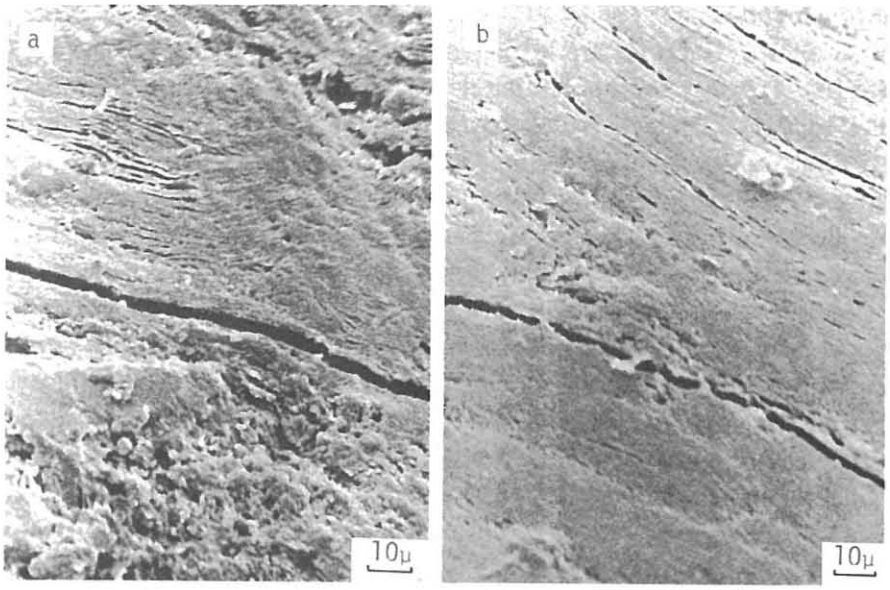

Fig. 5 Parallel cleavage fracture in feldspar grain (a), and in quartz grain (b).

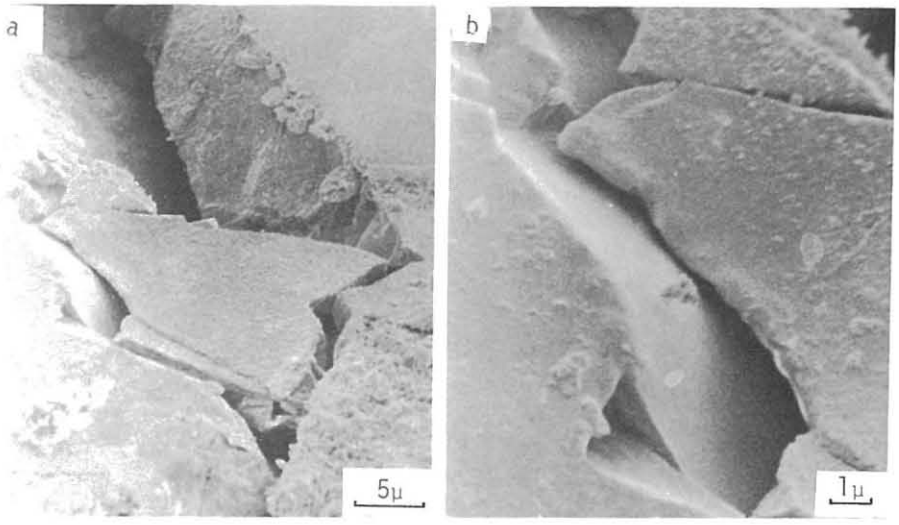

Fig. 6 Quasicleavage fracture in quartz grain (a), and its smooth and gentle swerved surface (b).

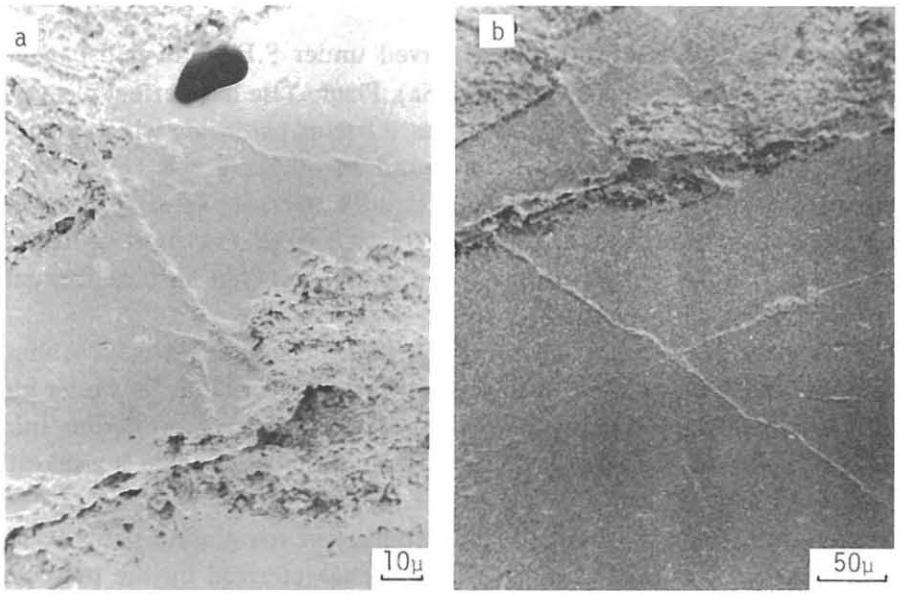

Fig. 7 shear fracture in quartz grain. The fracture with displacement along its plane (a) and a set of crossed fractures.

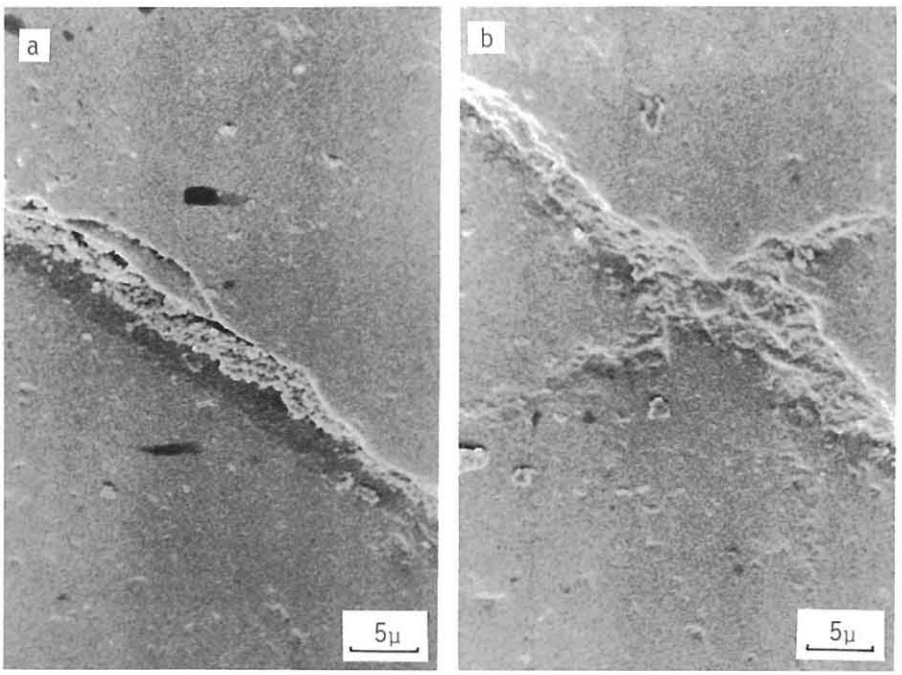

Fig. 8 The belt which consists of numerous minute fractures *en échelon* (a), and clossed belts (b).

Granite Pebble

Various types of fracture were observed under S.E.M. In feldspar grains, many parallel fractures were found (Fig. 5a). Plagioclase has perfect cleavage of {011} and twining plane (010), but it was difficult to decide which plane was fractured. Cleavage fracture was also found in quartz grains (Fig. 5b). This fracture develops linearly and has a smooth surface, so that it is easily distinguished from the normal rupture. Quasicleavage fracture was found in quartz grains (Fig. 6). This fracture has a gently swerved surface formed by high concentration of infinitesimal cracks.

Throughout the present observation, shear fracture traverses obliquely quartz grain and the grain was displaced by this fracture (Fig. 7). Under higher magnification, this fracture is seen as a belt consisting of numerous minute fractures *en échelon* (Fig. 8). In quartz, although the basal-plane is weakest, no basal-plane griding observed.

Normal and shear ruptures are predominant in the granite pebbles. Fig. 9 shows a surface of normal rupture which is characterized by the presence of *isometric dimples.* These are formed by development and connection of boids. Fig. 10 shows *elongated dimples* developed on the surface of shear rupture. Such elongated dimples may be formed as the result of sliding parallel to the shear stress.

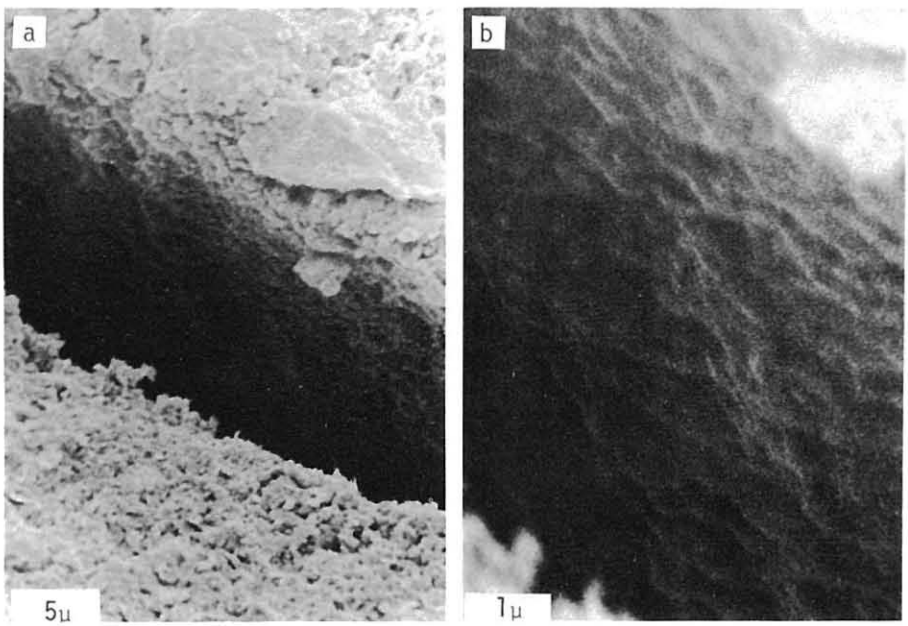

Fig. 9 A surface of normal rupture (a), and *isometric dimples* on the surface (b).

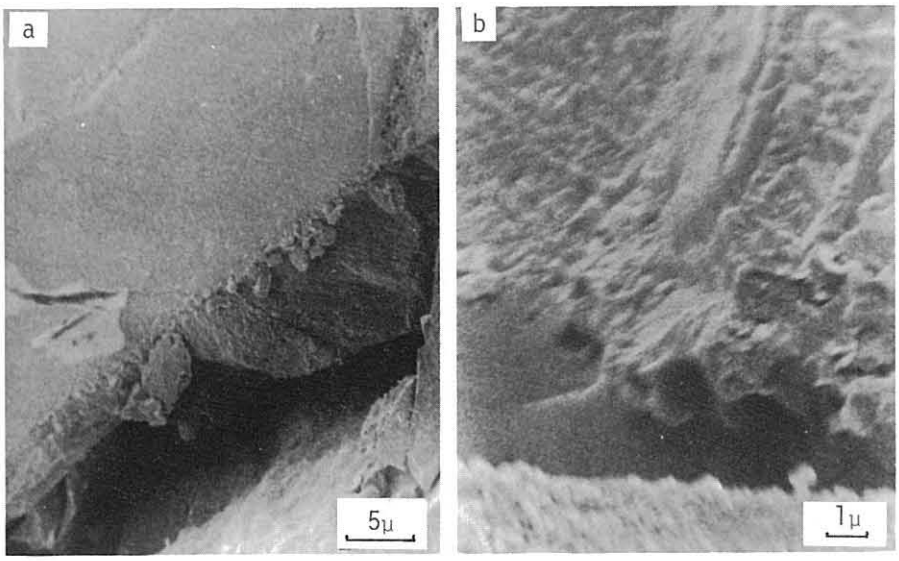

Fig. 10 A surface of shear rupture (a), and *elongated dimples* on the surface (b).

Discussion

It is clear that the type of fracturing in limestone pebble is entirely different from that in granite pebble. Microfracture in limestone pebble is more simple than in granite, in the latter fractures become complex by the combination of various types of fracture. This difference is probably caused by the following factors; intitial state of material, homogeneity of applied stress, presence of Griffith's *(potential)* cracks, mechanical properties of material, etc.

With regard to the initial state of material, limestone pebble was produced as a nodule, so that it is similar to a *clean material**. Granite pebble was, on the other hand, derived from its country mass and subjected to weathering during transportation and sedimentation. Therefore, this behaves as *dirty material*** (Fig. 11). Homogeneous microscopic structure of clean material behaves resistance against the generation of fractures, but heterogeneous distribution of impure grains causes less resistance.

Assumming that stress is applied homogeneously and that difference of initial state is negligible, the propaganda of fracture can be discussed. According to *the force-separation law* (Gilman, 1962), the value of critical

* *Clean material* consists of homogeneous sigle phase and when another phase is involved, it distributes homogeneously in the material.

** *Dirty material* involves heterogeneously many impure grains.

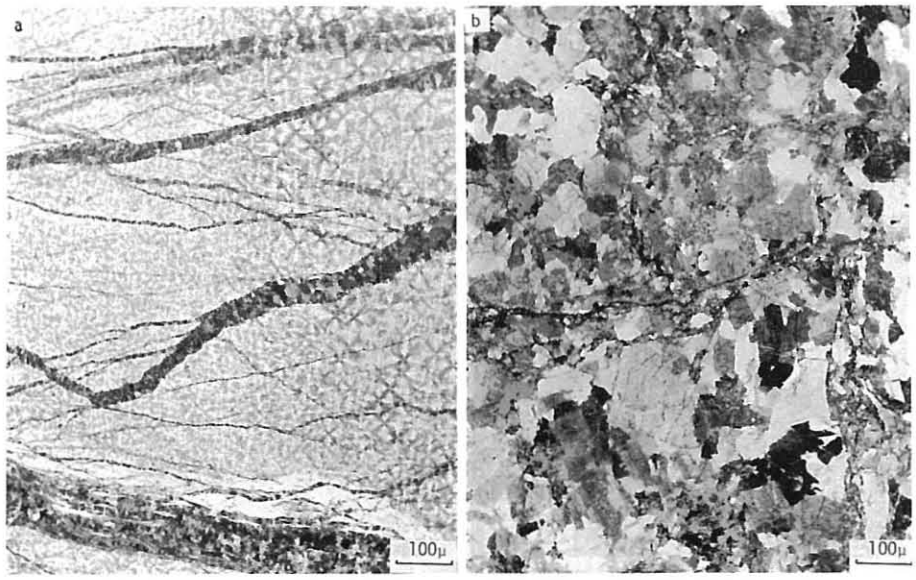

Fig. 11 Microphotograph of limestone pebble (a) and granite pebble (b).

strength, σ_c, is given as:

$$\sigma_c = \frac{E}{10}$$

and then, *the true surface energy*, γ_s, is given by

$$\gamma_s = \frac{E\, a_o}{20}$$

where E is Young's module and a_o is an equilibrate distance between atoms without stress (Appendix I).

If the yield strength, σ_Y, is larger than the bonded force (nearly equal to E/10), the material behaves as a perfect elastic body and the formulae given by Griffith (1924) can be applied, which gives a condition of fracture propaganda. If σ_Y is smaller enough compared to E/10, the fracturing generates plastically (Irwin, 1957). Without continuous cleavage fracture, the remaining types of fracture belong to the category of *local* plastic deformation. The local plastic flowage causes the increase of toughness (crack-resistance force of material). These relationship is shown in Fig. 12 (Appendix II). Fracture begins to propagate elastically under the condition of $C = C_F$ and then, it becomes dully at $C = C_x$ by the plastic deformation when $\gamma_p > \gamma_s$. The curved line DE in Fig. 12 shows the stress, σ_M, under the condition mentioned above. If σ (applied stress) remains constant during propaganda, even enough $C = C_x$, the fracture grows up because of $\sigma > \sigma_M$. However, if plastic work, γ_p, is large

enough and σ_M is shown as the curved line FG in Fig. 12, the fracturing becomes slow and stops at last.

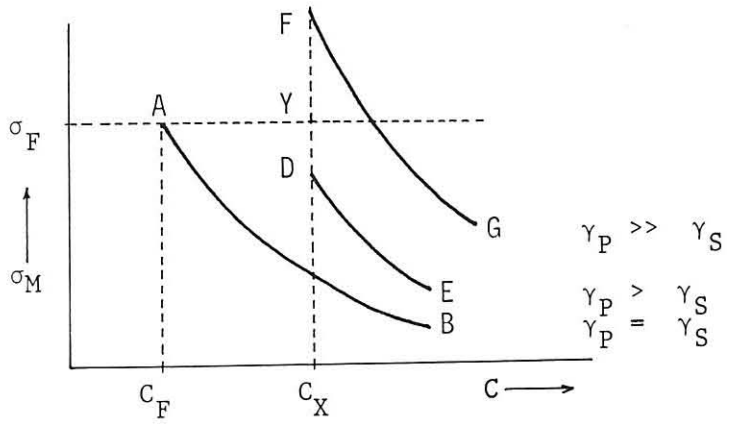

Fig. 12 An effect of plastic relaxation on plastic work, γ_p, according to the modification of Griffith's criterion.

On the basis of the result of observations and theoretical inquiry of fracture mechanics, following conclusion is given to the difference of megascopic features between limestone and granite pebbles. The difference of fracture type probably depends on the initial state of pebbles and generation of plastic deformation. In the case of limestone pebble, the fracture must be less developed due to the plastic relaxation at the apex of fracture, and because of *clean material.* On the other hand, granite pebble behaves as a brittle and *dirty material,* and involves many potential cracks. Therefore, fracture is well developed, forming various types of fracture.

In short, in limestone pebble, plastic relaxation occurs only at the apex of microfracture, and megascopic fracture is poorly developed. On the contrary, in granite pebble, elastic deformation occurs instead of plastic one, and megascopic fracture is well developed.

Acknowledgement

This paper is dedicated to Professor Kenzo Yagi on the occassion of his retirement from Hokkaido University, who has always encouraged us, postgraguate students. The present writer is greatly indebted to Prof. Yoshio Katsui and Dr. Kosuke Onuma of Hokkaido University for valuable suggestion and reading the manuscript. Particular thanks are also due to Mr. Norio Mino and Mr. Morio Akamatsu and their colleagues of the Historical Museum of

Hokkaido who kindly permit me to use the S.E.M., JEOL JSM-S1, and to Mrs. Setsuko Yokoyama of Hokkaido Univ. for typing the manuscript.

Appendix I

The fracture strength depends upon the bond strength between atom A and A′. In order to convert this bond strength to distance, a_0 is difined as equilibrate distance, a, between atoms without stress (Orowan, 1959). The stress, σ, needed to pull apart in a ($> a_0$) distance increases until reaching a critical strength, σ_c, and consequently the bond is distructed. At this time, an atom can be displaced even if the stress decreased. The curved line of stress-displacement can be approximated as a sinusoidal curve with wavelength, λ, and is given by

$$\sigma = \sigma_c \sin(2\pi x/\lambda) \tag{1}$$

where $x = a\text{-}a_0$ indicates the displacement from equilibrate position. When the displacement is an infinitesimal, the approximation for $\sin x \cong x$ can be permited, hence

$$\sigma \cong \sigma_c \cdot 2\pi x/\lambda$$

Assuming that this infinitesimal displacement obeys *the Hooke's low,* the equation on the stress-strain relation can be written as

$$\sigma = E \cdot C = \frac{Ex}{a_0}$$

therefore,

$$\sigma = \frac{\lambda}{2\pi} = \frac{E}{a_0} \tag{2}$$

In order to discribe the related equations for fracturing energy, *the true surface energy,* γ_s, (i.e. work done to form a new surface due to distruction of atomic bond) is defined as following equation (see Fig. 13):

$$2\gamma_s = \int_0^{\frac{1}{2}} \sigma_c \sin\left(\frac{2\pi x}{\lambda}\right) dx = \frac{\lambda \sigma_c}{\pi} \tag{3}$$

Therefore, from eq. (2),

$$\sigma_c = \sqrt{\frac{E\gamma_s}{a_0}}. \tag{4}$$

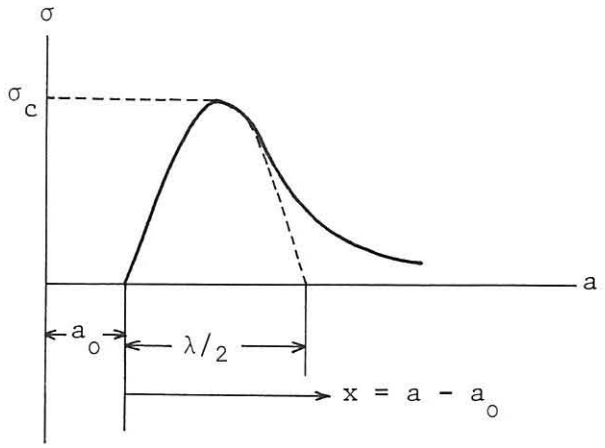

Fig. 13 The tensile stress needed to pull aprt in $a > a_0$ distance. a_0: the equilibrate distance between atoms at $\sigma = 0$. Fracturing occurs at $\sigma = \sigma_c$.

Appendix II

Let consider a small ellipse of fracture which has 2c in length. The maximum tensile stress, σ_{max}, is generated at the apex of fracture (Musknelishvili, 1953), and is written such as

$$\sigma_{max} = \left(1 + \frac{2C}{h}\right). \tag{5}$$

Stress is expressed by the curvature radius of fracture apex, ρ. Since ellipse has a curvature, $\rho = h^2/c$, σ_{max} is rewritten as

$$\sigma_{max} = \sigma + \left(1 + 2\sqrt{\frac{C}{\rho}}\right) \cong 2\sigma\sqrt{\frac{C}{\rho}}, \quad C \gg \rho$$

Therefore,

$$k\sigma = \frac{\sigma_{max}}{\sigma} = 2\sqrt{\frac{C}{\rho}} \tag{6}$$

indicates the coefficient of stress concentration at the infinite acute fracture.

A necessary condition of propaganda should be satisfied when the maximum tensile stress reaches the critical bond strength, σ_c. According to eqs. (4) and (6), a nominal stress, $\sigma = \sigma_F$, is given by

$$2\sigma_F\sqrt{\frac{C}{\rho}} = \sqrt{\frac{E\gamma_s}{a_0}}$$

namely,

$$\sigma_F \cong \sqrt{\frac{2E\gamma_s}{\pi C}\left(\frac{\rho}{3a_0}\right)}\ . \tag{7}$$

This relationship is only applied to perfect elastic body, hence σ_F indicates the fracturing stress (i.e. the load stress needed to generate complete fracture).

In plane-stress condition, the strain energy, W_E, is given by

$$W_E = \frac{\pi\sigma^2 C^2}{E} \quad . \tag{8}$$

Since an internal fracture is propagated symmetrically, two surface of 2c in length are formed and the surface energy, W_s, is given by

$$W_s = 2C\gamma_s \quad . \tag{9}$$

In this case, the Griffith criterion is rewritten from eqs. (8) and (9) as follows;

$$\frac{\partial}{\partial C}\left(\frac{\pi\sigma^2 C^2}{E}\right) \geqslant \frac{\partial}{\partial C}(4C\gamma_s)$$

therefore,

$$\sigma = \sigma_F = \sqrt{\frac{2E\gamma_s}{\pi C}} \quad . \tag{10}$$

When the plastic deformation occurs near the apex of fracture, plastic work, γ_p, must be done in addition to elastic work, γ_s, during fracture propaganda. Under the plane-stress condition, the Griffith's criterion must be modified as

$$\sigma_M = \sqrt{\frac{2E}{\pi C}(\gamma_s + \gamma_p)}$$

$$= \sqrt{\frac{2E\gamma_s}{\pi C}\left(1 + \frac{\gamma_p}{\gamma_s}\right)} \quad . \tag{11}$$

When $\gamma_p/\gamma_s > 1$, eq. (11) is simplified,

$$\sigma_M = \sqrt{\frac{2E\gamma_s}{\pi C}\left(\frac{\gamma_p}{\gamma_s}\right)} = \sqrt{\frac{2E}{\pi C}\gamma_p} \tag{12}$$

where σ_M indicates the stress needed to development of fracture. When the plastic deformation is generated near the apex, the fracture propaganda becomes dully and the concentrated stress is relaxed. This phenomenon can be easily understood when we compare eq. (7) to eq. (12), such as

$$\sqrt{\frac{2E\gamma_s}{\pi C}\left(\frac{\rho}{3a_0}\right)} = \sqrt{\frac{2E\gamma_s}{\pi C}\left(\frac{\gamma_p}{\gamma_s}\right)}$$

therefore,

$$\frac{\rho}{3a_0} = \frac{\gamma_p}{\gamma_s} \qquad (\gamma_p > \gamma_s) \cdot \qquad (13)$$

Reference

Girman, J.J., 1962. *Strength of ceramic crystals.* Am. Ceram. Soc. Caf., New York, 193p.

Griffith, A.A., 1924. Theory of rupture. *Proc. 1st Inter, Congr. Appl. Mech. Proc. Delft,* 55-63.

Irwin, G.R., 1957. Analysis of stress and strain near the end of a crack traversing a plate. *Jour. Appl. Mech.,* 24: 361-364.

Minoura, N., 1975. An electron microscopic study of th upper Pennsylvanian limestones of Kansas. *Jour. Fac. Sci. Hokkaido Univ., Ser.4,* 16: 196-330.

Muskhelishvili, N.I., 1953. *Some basic problems of the mathematical theory of elasticity.* 4th ed., Nordhoff, Groningen, 585p.

Orowan, E., 1959. Classical and dislocation theory of brittle fracture. In: *Fracture,* R.L. Averebach(ed.), John Wiley & Sons, Inc., New York, pp.147-160.

Telelman, A.S. and McEvily, A.J. Jr., 1967. *Fracture mechanics of structural materials.* John Wiley & Sons, Inc., New York, 348p.

Uda, T., 1973. Deformation of grante pebbles in "Utaro conglomerate" at Cape Erimo, Hokkaido, Japan. *Jour. Geol. Soc. Japan,* 79: 391-398.

Uda, T., 1976. Polyphase deformation of the Cape Erimo area by change of tectonic stress-field. *Jour. Geol. Soc. Japan,* 82: 1-18.

(Received on Oct. 31, 1977)